

Radon Transform based Local Tomography Algorithm for 3D Reconstruction

Kishore Rajendran and Karthikeyan B R

Abstract— An algorithm from Radon transform to obtain local tomography from multiple CT slices for localized 3D reconstruction is developed. The proposed method uses Radon transform to obtain projections for a region of interest. Reconstructing a particular cross section of a human body using local data will significantly reduce X-ray exposure during imaging. Image reconstruction is performed using filtered back projection technique. The property that distinguishes the developed algorithm from previous algorithms is the ability to track the Region of Interest (ROI) for every projection angle, computing projections along the lines intersecting the region of interest, and performing reconstruction using purely local data. Parallel beam projections are used and ROI is defined by a square or circular region. To reconstruct a local region of 20 pixel radius in a 256 x 256 image, 13% of the global data is required.

Keywords— Local tomography, Filtered back projection, Radon transform, Region of Interest

I. INTRODUCTION

Radon transform technique is well known for its application in Computerized Tomography (CT). In dimension two, and in any even dimension, Radon transform is not local and requires the knowledge of all projections of an image to reconstruct a particular region in the image [1]. Practically, this leads to global X-ray exposure on the patient during CT scan even if a small part of the patient's body is required for visualization. Thus, the ubiquitous goal of local tomography is to localize the imaging procedure to reduce radiation exposure and reconstruct the image without any declension in resolution.

Wavelet based local tomography techniques have been proposed by Farrokhi et.al [1], Destafano and Olson [2], and Delaney and Bresler [3]. Even though reduced exposure was exhibited in [2] and [3], the low resolution parts are recovered by global data measured at few angles [1]. Hence, these algorithms cannot accurately be termed as local tomography algorithms. Further reduction in exposure was exhibited by Olson in [4]. However, sparsely sampled non-local values are

utilized to obtain local tomography. A small number of line integrals that do not pass through the ROI are taken into consideration for localized reconstruction which results in unwanted exposure. In [1], local reconstruction of high resolution parts and low resolution parts of an image is achieved using only local measurements. The property of rapid decay of the Hilbert transform of ϕ for a scaling function (where $\hat{\phi}^{(j)}(0) = 0$ for $j = 1, 2 \dots K$ for some large K) is used which significantly results in reduced exposure and computations compared to the algorithms in [2] and [3], and reduced computations and greater exposure than [4]. The projections of the image along the lines intersecting the local ROI plus a small number of projections in the immediate vicinity are used to obtain a good approximation of the ROI in the reconstructed image.

In this paper, a Radon transform based spatial domain technique is developed to obtain local projections and to reconstruct the ROI using only the local projections. Hardware implementation is easier if only the local measurements are considered for reconstruction [1]. The main features of the developed algorithm are:

- It has reduced exposure compared to the algorithms cited in [1]-[3]. There is no necessity of obtaining projections that do not correspond to ROI as in [2] and [3]. Also, global estimates of projections are not required to reconstruct the local ROI. Projections are computed exclusively for ROI and the projections close to the ROI as used in [4] are not required.
- ROI can be a square or circular region located anywhere in the image.
- Computational complexity is less compared to other methods since purely local data is used for local reconstruction. Unlike in [3], Filters employed in filtered back projection algorithm are not angle dependant.

The organization of this paper is as follows. Section II contains a brief mathematical description of Radon transform and Interior Radon transform. Section III discusses the filtered back projection technique for image reconstruction along with the filters employed for the local reconstruction. Section IV illustrates the proposed local tomography algorithm. Significant difference in implementation steps between global and local tomography are also discussed. Section V discusses the simulation parameters and results. Section VI describes the 3D reconstruction of the local region obtained for multiple CT slices.

Manuscript submitted on February 8, 2012. This work was supported in part by M S Ramaiah School of Advanced Studies, Bangalore, India

Kishore Rajendran is with the Department of Electronics and Electrical Engineering, M S Ramaiah School of Advanced Studies, Bangalore, Karnataka 560058 India (Phone: +91-80-4906 5555; fax: +91-80-4211 1205; e-mail: kishore@msrsas.org).

Karthikeyan B R is with the Department of Electronics and Electrical Engineering, M S Ramaiah School of Advanced Studies, Bangalore, Karnataka 560058 India (e-mail: karthikeyan@msrsas.org).

II. PRELIMINARIES AND NOTATIONS

In this section, a brief description about the terminology and mathematical notations are given which are required in the subsequent subsections. All discussions in this paper are with respect to Cartesian coordinate system.

A. Radon Transform

Computerized Tomography involves the transmission of thin X-ray beams and detecting the loss in intensity of the transmitted beams for reconstructing the planar cross section of transmission media (human body). Given a 2D function $f(x,y)$ in Cartesian coordinates, the Radon transform of f can be defined as

$$R_\theta(x') = \int_{-\infty}^{\infty} f(x', y') \Big|_{\substack{x' = x \cos \theta + y \sin \theta \\ y' = -x \sin \theta + y \cos \theta}} dy' \quad (1)$$

where $\theta \in [0 \text{ to } \pi]$. Eq. (1) represents the line integrals of the function f parallel to the y' . The line can be related to the X-ray path and the line integral for a particular line can be related to the sum of different densities or attenuation coefficients μ along the X-ray beam's line of travel. The relation between Radon transform and the attenuation profile with respect to difference in beam intensities can be established as [6]:

$$R_\theta(x') = \ln \left(\frac{I_0}{I_t} \right) \quad (2)$$

where I_0 is the intensity of the incident X-ray beam and I_t is the intensity of the detected X-ray beam after transmission.

B. Interior Radon Transform

The Interior Radon transform is the restriction of Radon transform to the lines passing through the ROI of a function f , which is a circle of radius $a(a < 1)$ with respect to the origin [1]. It is defined by

$$R_\theta f(s) = R_\theta f(s) 1_{[-a,a]}(s) \quad (3)$$

where, $R_\theta f(s)$ is the Radon transform of a function f . Recovering the function f from the interior Radon transform is called the interior radon transform or region of interest tomography [1]. The interior Radon transform is an incomplete data problem [5].

III. IMAGE RECONSTRUCTION

The 1D Fourier transform of $R_\theta(x')$ is given by [7]

$$F_\theta(\omega) = \frac{1}{N} \int_{-\infty}^{\infty} R_\theta(x') e^{(-i \frac{2\pi}{N} \omega x')} dx' \quad (4)$$

where $F_\theta(\omega)$ is the Fourier transform of the projection at frequency ω . Reconstructing the function f from the 1D Fourier transform of $R_\theta(x')$ is known as the Fourier slice theorem or Central slice theorem.

The Fourier transform of the projection data $F_\theta(\omega)$ is multiplied with a filter function $H(\omega)$ as

$$G_\theta(\omega) = F_\theta(\omega) H(\omega) \quad (5)$$

where, The filter $H(\omega)$ can be a ramp function given by $|\omega|$ or

the Shepp-Logan function given by [7]

$$H(\omega) = \left[|\omega| \frac{\sin(\omega)}{\omega} \right] \quad (6)$$

The 1D inverse Fourier transform of $G_\theta(\omega)$ is given by

$$\hat{R}_\theta(x') = \int_{-\infty}^{\infty} G_\theta(\omega) e^{(i \frac{2\pi}{N} \omega x')} d\omega \quad (7)$$

In Eq. (7), $\hat{R}_\theta(x')$ is the filtered projection at angle θ . The reconstruction is obtained by back projecting $\hat{R}_\theta(x')$ at all θ to obtain a good approximation of the function $f(x,y)$.

$$\hat{f}_\theta(x, y) = \hat{R}_\theta(x) \forall x \quad (8)$$

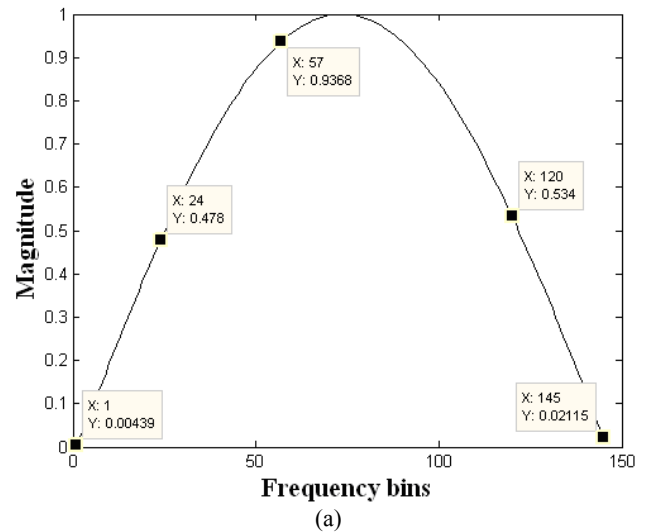
$$S(x, y) = \int_0^{2\pi} \hat{f}_\theta(x, y) d\theta \quad (9)$$

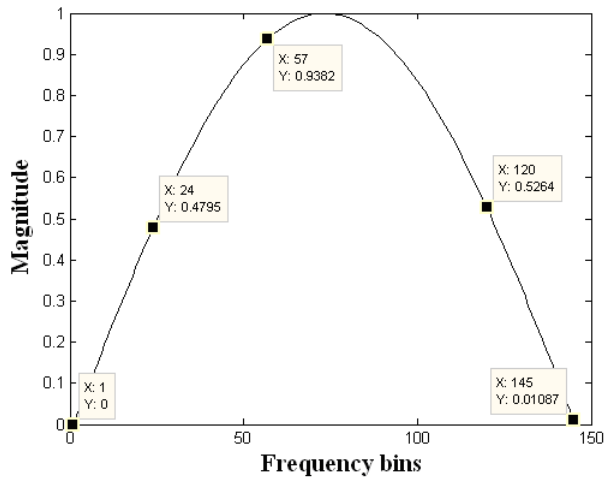
A filter that provides good results in filtered backprojection during local reconstruction is the cosine filter defined by

$$H(u) = \sin \left(\frac{2\pi}{f_s} u \right) \quad (10)$$

for $0 \leq u \leq M-1$ and $f_s = 2M-1$, where M is the length of discrete samples contained in $R_\theta(x')$.

The magnitude responses of Shepp-Logan and Cosine filters are shown in Fig.1 for an arbitrary value $M=145$. The filter responses appear similar with fractional change in the magnitude, but the filters yield significant changes during reconstruction.





(b)

Fig. 1 Filter Response of 1D Filter (No. of Frequency Bins = 145) (a) Shepp Logan (b) Cosine

The PSNR obtained using Shepp Logan and Cosine filters are closely similar (difference of ± 0.50 PSNR and ± 0.0020 MSE) with Shepp Logan providing better quantitative results and Cosine filter providing better visually qualitative results during global and local reconstruction.

IV. LOCAL TOMOGRAPHY ALGORITHM

The local tomographic reconstruction is obtained for a defined ROI from the global function $f(x,y)$. The ROI can be either a square/rectangular or circular region. The square ROI can be defined by representing the four corner coordinates and the circular ROI is defined by the coordinates of its origin and a radius large enough to encompass the ROI.

Given a local set of points $f_L(x,y)$ (ROI) in a 2D entity $f(x,y)$ as shown in Fig. 2, the Radon transform corresponding to the ROI can be expressed as

$$R_\theta(x') = \int_{-\infty}^{\infty} f_L(x', y') \Big|_{\substack{x' = x \cos \theta + y \sin \theta \\ y' = -x \sin \theta + y \cos \theta}} dy' \quad (11)$$

where $\theta \in [0 \text{ to } \pi]$. Eq. (11) represents the line integrals parallel to the y' axis intersecting the ROI from the global function for angle θ .

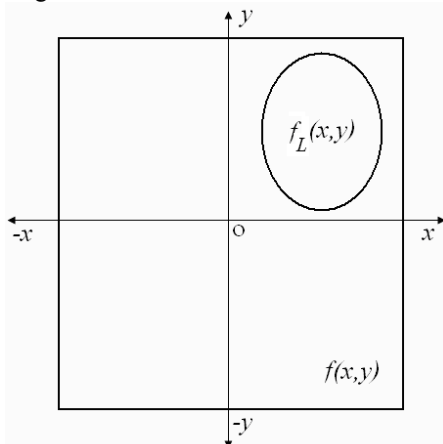


Fig. 2 Local region $f_L(x,y)$ in a 2D function $f(x,y)$

Fig.3 illustrates the difference between global and local tomography using parallel beam projections.

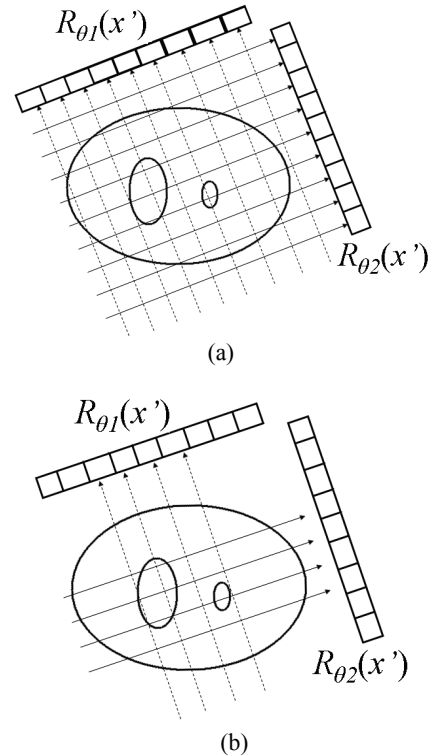


Fig. 3 (a) Global tomography (b) Local tomography

The ROI in the image is defined by a circle defined by its origin and radius. The ROI and its circumferential coordinates are subjected to change for every θ and hence computed for every θ using the Given's rotation formula [8]. The new x coordinates of the ROI are calculated before computing the projection. Knowing the transformed coordinates corresponding to the ROI, the projections are computed only for the area under the ROI. At every θ , the ROI remains a circular region and projections for areas outside the ROI are unnecessary.

If $R_\theta(x')$ is the global Radon transform for any θ , then the local region in projection axis is $x'_L \in x'$. The local projection $R_\theta(x'_L)$ as a subset of $R_\theta(x')$ for a given θ is illustrated in Fig.4.

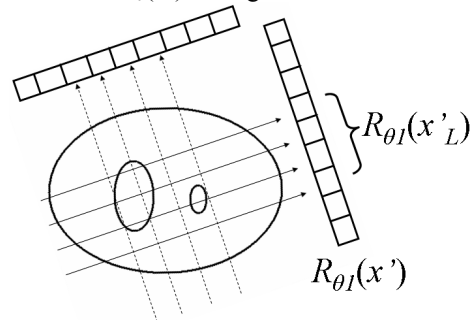


Fig. 4 Local projections $R_\theta(x'_L)$ for a particular θ
The projection for a given θ can be computed for a local

region ranging from x'_{Lmin} to x'_{Lmax} where x'_L is the transformed local x coordinates from $f_L(x,y)$. The projections that do not correspond to the ROI are assumed to be zero as shown in Fig.5.

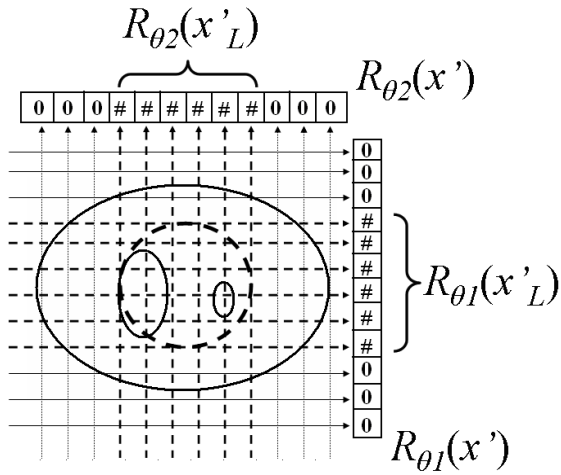


Fig. 5 Local projections for the highlighted circular ROI. Nonlocal projections are assumed to be zero.

The projections are subjected to filtered back projection using Cosine filter. Filtered back projection can be implemented locally or globally. Global filtered back projection employs angle independent filters. In this case, the local projections with nonlocal projections assumed to be zero is considered. Local back projection involves ROI dependant filters for circular ROI and angle dependant filters for square ROI. The simulation carried out in this paper for the different test cases uses global back projection for local tomography.

V. SIMULATION PARAMETERS

The simulations were performed on MATLAB software version r2007b. Test case 1 is the Shepp Logan phantom image used as the input for the developed local tomography algorithm. The image size is 201 x 201 and the ROI is defined as a circle with the origin at (-1, 19) and a radius of 50 pixels. A total number of 181 projections were computed with θ varying from -90 to 90 degrees in steps of 1 degree increments. The results of local tomography algorithm using Cosine filter in the back projection algorithm and global tomography using Shepp- Logan filter in back projection algorithm are shown in Fig.6.

Test case 2 is a head CT image of size 209 x 209. The circular ROI is defined by its origin at (-5, 23) with radius 50 pixels. The results obtained for global and local reconstruction is shown in Fig. 7.

If the ROI is square region defined by the corner coordinates, the ROI is considered to be a small image inside the global plane. The two extremities of the ROI at any given θ will be any two of the four transformed x coordinates of the corners of square. The results of local tomography using a square ROI for test case 2 is shown in Fig. 8.

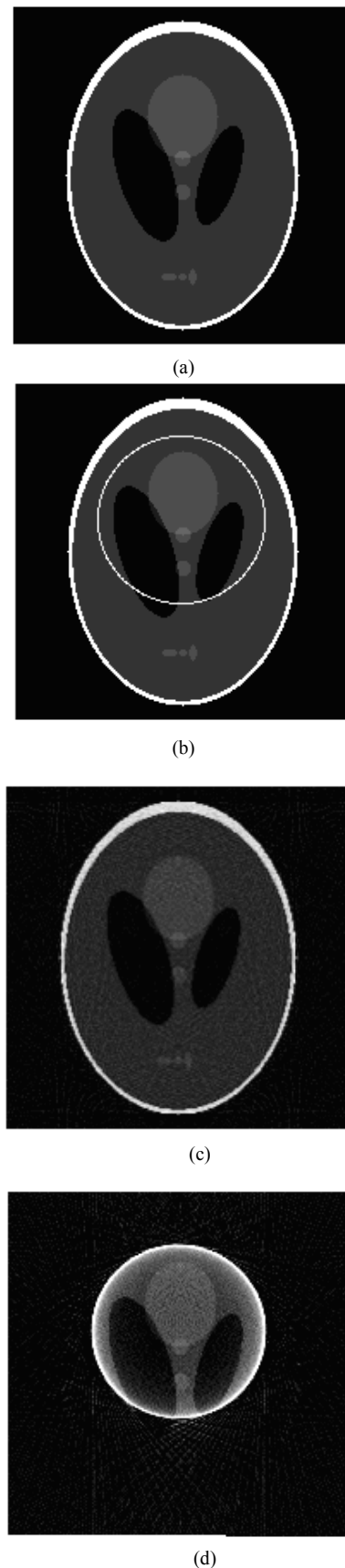
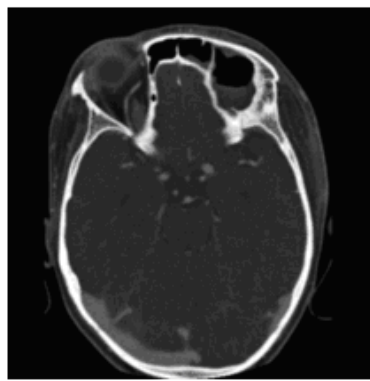
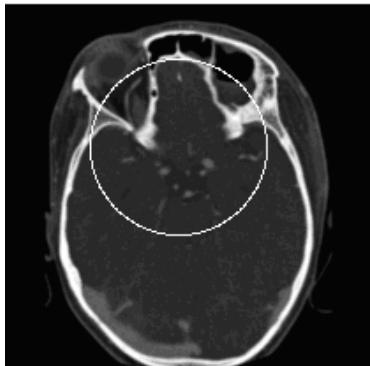


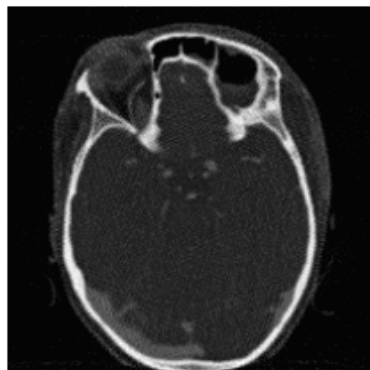
Fig. 6 (a) Input Phantom image (b) ROI of 50 pixel radius defined in the image (c) filtered back projection using Shepp Logan filter (d) filtered back projection using Cosine filter



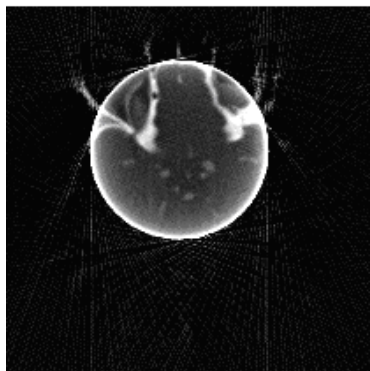
(a)



(b)

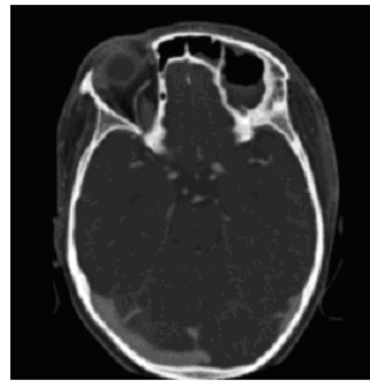


(c)

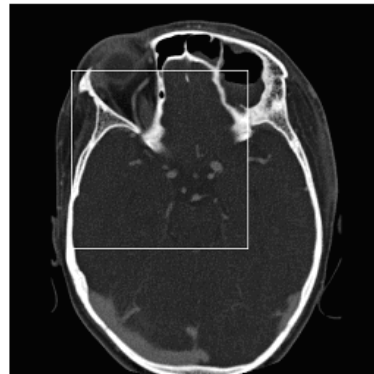


(d)

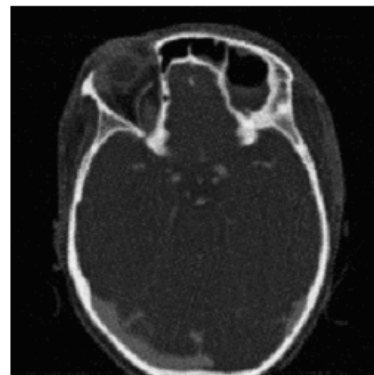
Fig. 7 (a) Input Head CT image (b) Defined circular ROI of 50 pixel radius (c) Global reconstruction Shepp Logan filter (d) Local reconstruction using Cosine filter



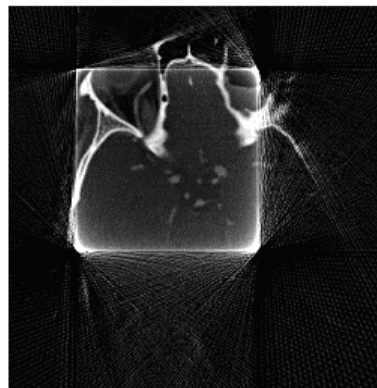
(a)



(b)



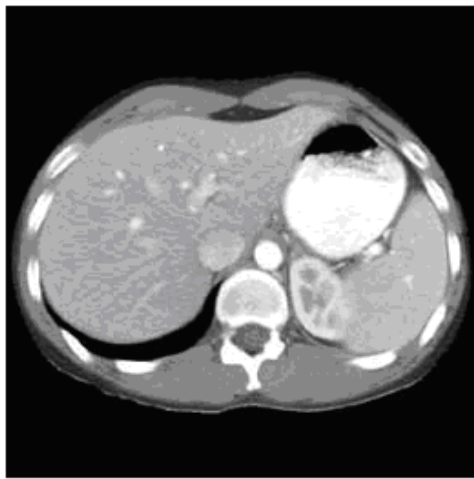
(c)



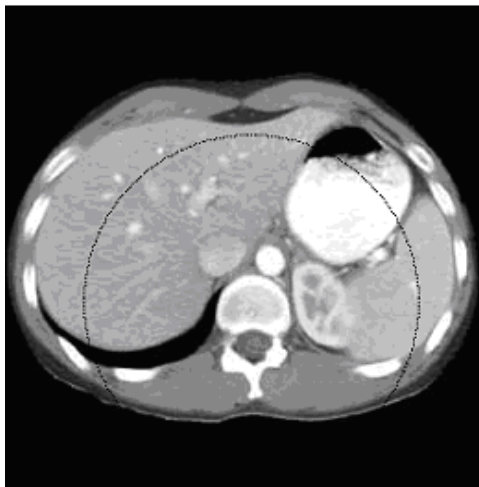
(d)

Fig. 8 (a) Input Head CT image (b) Defined square ROI of side 199 pixels (c) Global reconstruction Shepp Logan filter (d) Local reconstruction using Cosine filter

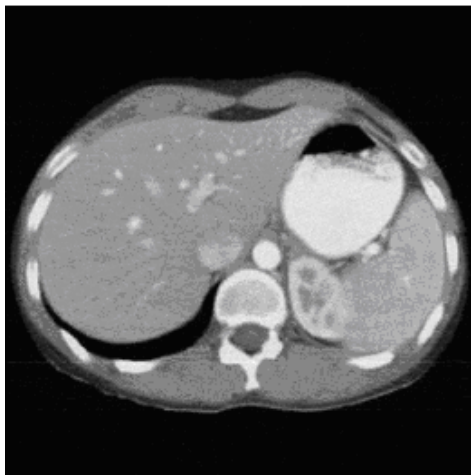
Test case 3 is an abdomen CT image of size 289 x 289. Significant areas of the image correspond to soft tissues showing high intensity levels. The circular ROI is defined by its origin at (6, -37) with radius 100 pixels. The results obtained for global and local reconstruction is shown in Fig.9.



(a)



(b)



(c)



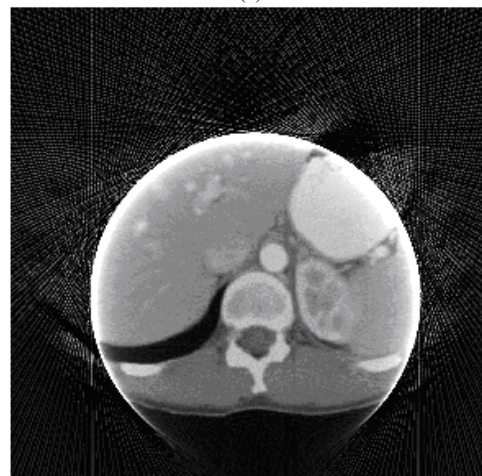
(d)

Fig. 9 (a) Input Abdomen CT image (b) Defined circular ROI of 100 pixel radius (c) Global reconstruction Shepp Logan filter (d) Local reconstruction using Cosine filter

The results obtained from local tomography using cosine filter exhibits better visual results compared to the results obtained from Shepp-Logan filter and Ram-Lak filter. The comparative results for test case 3 are shown in Fig. 10.



(a)



(b)



(c)

Fig. 10: Local reconstruction using (a) Shepp Logan filter (b) Ram-Lak filter (c) Cosine filter

The developed local tomography algorithm utilizes purely local data and hence the exposure is reduced compared to global tomography. The percentage of exposure for an image of size 256 x 256 subjected to the developed local tomography algorithm is tabulated for different ROI radii with respect to global reconstruction in Table I. The exposure parameters will be slightly higher for square ROI.

Irrespective of the ROI size and type, exposure is calculated using the formula:

$$\%Exposure = \frac{\sum_{\theta=0}^{\pi} n_L(\theta)}{\sum_{\theta=0}^{\pi} n_G(\theta)} \times 100 \quad (12)$$

where, $n_L(\theta)$ is the number of samples present in local projection $R_{\theta}(x'_L)$ and $n_G(\theta)$ is the number of samples present in global projection $R_{\theta}(x')$ for a particular θ which is given by:

$$n_G(\theta) = \left[\frac{x'_{\max}(\theta) - x'_{\min}(\theta)}{\Delta x'} \right] + 1 \quad (13)$$

$$n_L(\theta) = \left[\frac{x'_{L\max}(\theta) - x'_{L\min}(\theta)}{\Delta x'_L} \right] + 1 \quad (14)$$

Here the distance between the incident beam is unit distance and equally spaced, $\Delta x' = \Delta x'_L = 1$.

TABLE I
PERCENTAGE OF EXPOSURE FOR DIFFERENT ROI RADIUS

ROI Radius (pixels)	% of exposure with respect to global tomography for the developed algorithm	% of exposure with respect to global tomography in [1]
16	10.10	22
20	12.55	25
25	15.61	28.75
35	21.74	36.25
50	30.92	47.50

VI. 3D LOCAL RECONSTRUCTION

Diagnostic Radiology widely employs volumetric models generated from multiple slices of CT images. In case of tumor surgery, 3D volumetric rendering helps in identifying the dimensions and location of the tumor. In [9], cranial vault reconstruction using 3D models obtained from CT slices for implant design and presurgical training is exhibited.

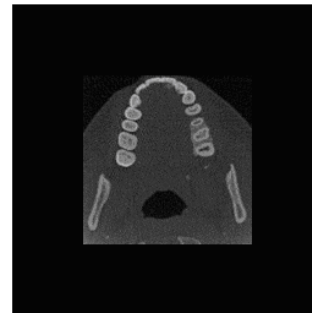
The local tomography algorithm can be implemented on a particular area of interest with apriori knowledge of the organ/tissue's anatomical location. Multiple slices of local tomography will result in localized volumetric reconstruction. Test case 4 shown in Fig.11(a) corresponds to head CT. It is subjected to the developed local tomography algorithm for a square ROI. The resulting image contains residual whitening at the boundaries of the ROI. The whitening is removed by cropping the locally reconstructed image as shown in Figure Fig.11(b). The same procedure is applied for the entire CT image data set comprising of 166 images.

A. 3D Reconstruction by Thresholding

MIMICS[®] software (Materialise Inc.) was used for the 3D reconstruction. The threshold for a particular image region with particular image intensity is set which is adapted for the entire dataset and the 3D model for the thresholded region is generated. The region of interest for the image as shown in Figure 11(b) is a square encompassing the mandible and the maxilla. The ROI is defined to perceive the region corresponding to the anatomical area of interest from all slices when subjected to local tomography.



(a)



(b)

Fig. 11 (a) Global Image (b) Local image after removing the noisy borders

The global and local intensity thresholding, and 3D reconstruction for the test case 4 are shown in Fig.12 and Fig.13 respectively.

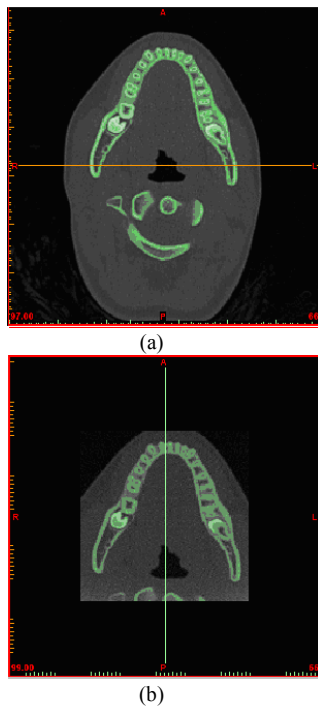


Fig. 12 Thresholding for (a) global image (c) local image

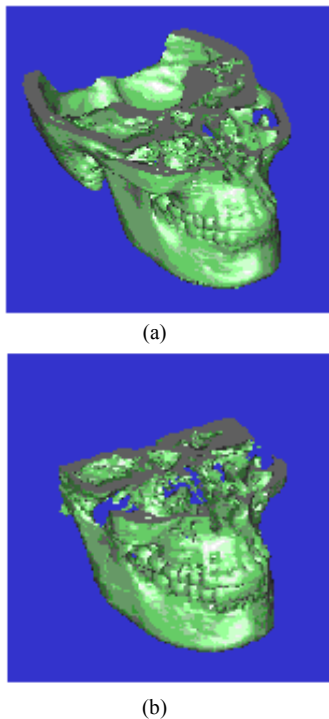


Fig. 13 3D (a) Global reconstruction (b) Local reconstruction

VII. CONCLUSION

The developed local tomography algorithm exhibits reduced exposure compared to the other local tomography techniques cited in the literature. Based on the observation, Cosine filter provides better results in cases of local tomography compared to Shepp Logan filter. Radon transform can be localized along any one dimension x or y assuming that the non-local projections are zero for all θ . The filtered back projection technique can be localized which employs filter whose length

is dependent on ROI size and projection angle (if square ROI is involved). This in turn intensifies the computational complexity. Further emphasis will be on removal of the ROI residual noise during filtered back projection. Localized filtered back projection has found to reduce the white residues and testing and validation is being carried out as a future work.

REFERENCES

- [1] F.R. Farrokhi, K.J. Ray Liu, C.A. Berenstein and D. Walnut, "Wavelet based Multiresolution Local Tomography", *IEEE Trans. Image Processing*, vol.6, No.10, pp. 1412-1430, 1997.
- [2] J. Destafano and T. Olson, "Wavelet localization of the Radon transform," *IEEE Trans. Signal Processing*, vol. 42, pp. 2055 – 2067, Aug. 1994.
- [3] A. H. Delaney and Y. Bresler, "Multiresolution tomographic reconstruction using wavelets," *IEEE Trans. Image Processing*, vol. 4, No.6, pp. 799-813, June 1995.
- [4] T. Olson, "Optimal time-frequency projections for localized tomography," *Ann. Biomed. Eng.*, vol. 23, pp. 622-636, Sept. 1995.
- [5] F. Natterer, *The Mathematics of Computerized Tomography*, New York: Wiley, 1986.
- [6] J. T. Bushberg, J. A. Seibert, E.M. Leidholdt Jr. and J. M. Boone, *The Essential Physics of Medical Imaging*, Philadelphia: Lippincott Williams and Wilkins, 2002.
- [7] A. M. Ali, Z. Melegy, M. Morsy, R. M. Megahid, T. Bucherl and E. H. Lehmann, "Image reconstruction techniques using projection data from transmission method," *Ann. Nuclear Energy*, vol.31, pp.no. 1415 – 1428, 2004.
- [8] G. H. Golub and C. F. Van Loan, *Matrix Computations*, The John Hopkins University Press, 1989.
- [9] P. K. Patel, L. Ahao, D. E. Morris and P. VM. Alves, "Our Experience with Virtual Craniomaxillofacial Surgery: Planning, Transference and Validation," *Proceedings of Medicine Meets Virtual Reality 16*, Vol. 132, pp.no. 363-365, 2008.